ARCHIVES
of
FOUNDRY ENGINEERING

ISSN (2299-2944)
Volume 2026
Issue 3/2026

144 – 152

18/3

10.24425/afe.2026.158029

Published quarterly as the organ of the Foundry Commission of the Polish Academy of Sciences

# The Complex Computational System for Simulating the Carbonitride Precipitation Process and Precipitate Microstructure in Microalloyed Steels

**P. Marynowski *, M. Hojny**
AGH University of Krakow, Poland
* Corresponding author. e-mail address: pmarynow@agh.edu.pl

Received 05.05.2026; accepted in revised form 14.09.2026; available online 30.10.2026

## Abstract

Microalloying elements such as Nb, V or Ti are added to steels to improve their mechanical properties through precipitation strengthening and grain refinement. Due to the strong chemical affinity of these elements for interstitial elements (C, N), nitrides, carbides or products of their mutual solubility, carbonitrides may form. The basic stereological parameters of precipitates, such as size, $r$, and volume fraction, $V_v$, play a key role in determining the strengthening effect and consequently influence the mechanical properties of steel. The complex computational system for simulating the carbonitride precipitation process was developed and implemented. One of the most important modules of the system enables simulation of the precipitate microstructure in microalloyed steels and calculation of the stereological parameters of precipitates. The obtained results provide quantitative information on the carbonitride precipitation process and the stereological parameters of precipitates, which may be used as input data for further mechanical property modelling. The developed computational system is described and validated through comparison with experimental observations.

**Keywords:** Microalloyed steels, Microstructure, Mechanical properties, Precipitates, Carbonitrides

## 1. Introduction

In technical applications of metal alloys, iron alloys (structural steels) play a crucial role. Among structural steels, microalloyed steels with a ferritic-pearlitic structure are the largest group. They are characterised by high mechanical strength, good weldability and ductility. The basic requirements for microalloyed steels are a high yield strength, $R_{p0.2}$ in the range of 450–600 MPa, good ductility, crack resistance and good weldability (when the carbon content is between 0.02% and 0.2%). High yield strengths above 600 MPa are required when discussing advanced high-strength microalloyed steels. Due to high mechanical properties, achieved only by small additions of microadditives introduced separately or comprehensively [1], these steels are increasingly used in industries such as defence sector, where high mechanical properties are particularly important. The strong chemical affinity of microalloying elements such as Ti, Nb or V for interstitials elements (C, N) results in the formation of binary compound, nitrides, carbides or products of their mutual solubility, carbonitrides, M(C,N). The mechanical properties of microalloyed

© The Author(s) 2026. Open Access. This article is licensed under a Creative Commons Attribution 4.0 International License (http://creativecommons.org/licenses/by/4.0/), which permits use, sharing, adaptation, distribution and reproduction in any medium or format, as long as you give appropriate credit to the original author(s) and the source, provide a link to the Creative Commons licence, and indicate if changes were made.

steels are significantly affected by carbonitride precipitation, which contributes to the precipitation strengthening effect and grain refinement. The size and distribution of precipitates are significantly influenced by the chemical composition of the steel and processing parameters, such as the cooling rate from the austenitising temperature, the temperature and duration of isothermal holding. The chemical composition of austenite at a given temperature is determined by the conditions of thermodynamic equilibrium. The size distribution of precipitates is an important parameter affecting the precipitation strengthening effect and the final mechanical properties of the steel after the manufacturing process. In austenite, precipitates can influence austenite grain growth, whereas in ferrite they contribute to precipitation strengthening effect.

Some thermodynamic models to calculate the chemical composition of austenite and carbonitrides was developed [2-6]. All of them are based on the regular solution model for stoichiometric phases proposed by Hillert and Staffansson [7]. Thermodynamic models of carbonitride precipitation under equilibrium conditions allow the determination of the equilibrium volume fraction and chemical composition of undissolved precipitates, as well as the chemical composition of the austenite matrix. These models are based on thermodynamic calculations of systems comprising iron, microalloying elements (V, Nb, Ti, Zr and Al) and carbon and/or nitrogen. The Adrian model is one of the advanced thermodynamic models developed for describing the precipitation of microalloying elements in the form of carbides, nitrides and carbonitrides [2]. Adrian's work contains a description of thermodynamic models for the precipitation of simple compounds, such as carbides and nitrides, as well as complex carbonitrides. A series of models have been developed to calculate the kinetics of the precipitation process from supersaturated solutions, based on the model developed by Kampmann and Wagner [8] (KWN). The KWN model is based on the classical theory of nucleation, growth and coarsening, allowing the simultaneous description of nucleation, growth and coarsening processes during precipitate evolution. Combined with accurate thermodynamic functions, the KWN approach enables a quantitative description of precipitate evolution as a function of time, including their size distribution and stereological parameters. Recent advances in the use of computational power have significantly contributed to research on its application in the simulation of physical phenomena. The high computational speed and the modern possibilities of numerical tools, enable the modelling of phenomena during the carbonitride precipitation process. In response to the growing demand for high strength low alloyed steels (HSLA), the complex computational system includes a proprietary solution for kinetic and thermodynamic models, based on a hybrid combination of the two existing Maugis-Gouné and Adrian models [9], which are considered to be among the most advanced approaches for describing carbonitride precipitation process, has been developed. General information concerning the carbonitride precipitation process in steels has been reported in [7,10]. One of the key modules of the system enables the simulation of the evolution of precipitate microstructures in microalloyed steels and the determination of their stereological characteristics. The obtained results provide quantitative information on carbonitride precipitation behaviour, including precipitate characteristics, which can be used as input data for further modelling of mechanical properties. The developed computational system is described and validated by comparison with experimental observations. The experimental verification presented in this work is focused on the validation of the precipitation model and predicted precipitate characteristics, rather than on the direct prediction of mechanical properties.

# 2. Kinetic and thermodynamic models

The kinetic model implemented in the complex computational system is based on the **C**lassical **T**heory of **N**ucleation and **G**rowth (CTNG). The model describes changes in the free energy, ΔG, associated with the formation of embryos in a supersaturated solid solution. The precipitation process is divided into three stages: nucleation, growth and coarsening, which can occur simultaneously. A detailed description of this model is presented in [11]. The most important equations are presented below. The chemical composition of the outer layer of carbonitride $MC_yN_{1-y}$ can be calculated from a system of nonlinear equations [7,11-12]:

$$\begin{cases} ln\frac{y_i K_{MC(r)}}{X_M^i X_C^i} + (1-y_i)^2\frac{L_{CN}}{RT} = 0 \\ ln\frac{(1-y_i)K_{MN(r)}}{X_M^i X_N^i} + {y_i}^2\frac{L_{CN}}{RT} = 0 \\ D_C\left(Y_C^i - Y_C\right) = y_i D_M(Y_M^i - Y_M) \\ D_N\left(Y_N^i - Y_N\right) = (1-y_i)D_M(Y_M^i - Y_M) \end{cases} \quad (1)$$

*where: $Y_{M,C,N}$ - the atomic fractions dissolved in the matrix, $Y_{M,C,N}^i$ - the atomic fractions at the matrix–precipitate interface. $D_{M,C,N}$ - the diffusion coefficients in the matrix. $L_{CN}$ - the interaction parameter. $K_{MC}(r)$ and $K_{MN}(r)$ - the solubility products.*

The system of equations (1) describes the approximate thermodynamic equilibrium at the matrix-precipitate interface and the equality of atomic fluxes, $J$ of elements diffusing into the precipitate layer:

$$\begin{cases} J_C = y_i J_M \\ J_N = (1-y_i)J_M \end{cases} \quad (2)$$

Because the diffusion coefficients of interstitial elements, C and N, are significantly higher than those of substitutional elements, M, it can be assumed that the concentrations of C and N in the precipitate layer are equal to their concentrations in the matrix.

$$Y_C^i = Y_C \; and \; Y_N^i = Y_N \quad (3)$$

$$\begin{cases} \frac{y_i K_{MC}(r)}{Y_M^i Y_C} = e^{-(1-y_i)^2\frac{L_{CN}}{RT}} \\ \frac{(1-y_i)K_{MN}(r)}{Y_M^i Y_N} = e^{-{y_i}^2\frac{L_{CN}}{RT}} \end{cases} \quad (4)$$

From the system of equations (4), $Y_M^i$ is calculated from the first equation of the system.

$$Y_M^i = \frac{y_i K_{MC}(r) e^{(1-y_i)^2\frac{L_{CN}}{RT}}}{Y_C} \quad (5)$$

Substituting this result into the second equation yields a nonlinear equation that allows the value of $y_i$ to be calculated.

$$f = y_i\left(Y_N K_{MC}(r) e^{(1-2y_i)\frac{L_{CN}}{RT}} + Y_C K_{MN}(r)\right) - Y_C K_{MN}(r) = 0 \quad (6)$$

To solve the nonlinear equation, the Newton method is applied using the general form:

$$x_{n+1} = x_n - \frac{f(x_n)}{f'(x_n)} \quad (7)$$

The derivative of equation (7) is given by:

$$\frac{df}{dy_i} = Y_N K_{MC}(r) e^{(1-2y_i)\frac{L_{CN}}{RT}} + Y_C K_{MN}(r) - 2y_i^2 \frac{L_{CN}}{RT} Y_N K_{MN}(r) e^{(1-2y_i)\frac{L_{CN}}{RT}} \quad (8)$$

After calculating the value of $y_i$(within the interval (0,1)), the sought value of $Y_M^i$is determined from equation (5).
The presented equations were implemented in the cellular automata module of the computational system to simulate the carbonitride precipitation process, generate images of precipitate distributions, and calculate the stereological parameters of precipitates.

# 3. General assumption of the complex computational system

The complex computational system (**Fig. 1**) enables the accelerated development and optimization of new steel grades by allowing changes in chemical composition and processing parameters. The system consists of several integrated modules that together form a coherent computational framework. The main modules include:

1. Pre/Postprocessor (interactive graphical interface).
2. Thermodynamic model (e.g. chemical composition of precipitations).
3. Kinetic model (e.g. the mean radius of precipitations).
4. Cellular automata (CA) model for simulating the spatial distribution of carbonitride precipitates and generating two-dimensional images for comparison with experimental observations.

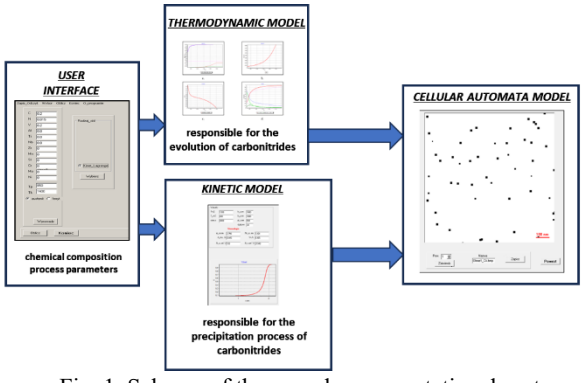



Fig. 1. Scheme of the complex computational system

One of the key modules of the complex computational system is the module responsible for the simulation and visualization of carbonitride precipitate distributions. The two-dimensional representation of precipitate microstructure is generated using the Cellular Automata (CA) model. The computational domain is divided into individual cells, each assigned a specific state: (1) matrix phase (austenite/ferrite), (2) precipitate, and (3) precipitate boundary. Each cell contains internal variables, including spatial coordinates $(x, y, z)$, parameters related to precipitate radius, local concentrations of C, N and microalloying elements. Based on predefined transition rules, the state of the automaton evolves by updating individual cell states during subsequent time steps. After completion of the simulation, the final automaton state is used to generate the precipitate distribution and calculate stereological parameters. The CA model consists of cubic cells arranged in a three-dimensional space. The computational domain is defined by dimensions $\Delta x, \Delta y$, and $\Delta z$. A cross-sectional plane $pl_z$and a layer with thickness $2d_{pl_z}$are selected, within which precipitate nuclei located near the observation plane are generated. The model represents precipitates using discrete cells. Therefore, their geometrical appearance results from the adopted cellular discretization rather than their actual physical shape. A Moore neighbourhood was selected, meaning that all cells located along the edges and at the corners of a given cell are considered neighbouring cells. Each automaton cell contains variables defining its state and interactions with neighbouring cells during subsequent time steps. These variables include the coordinates $(x, y, z)$ of the cell centre, cell state information (matrix phase, precipitate or precipitate boundary), cell size, local concentrations of M, C and N, and the cell identification number. Based on the calculated maximum number of nuclei at a given time step, precipitate nuclei are randomly generated within the computational domain and their states are updated accordingly. Cells that have already become nuclei are excluded from further random selection. Using parameters obtained from the precipitation kinetics model, including the current matrix composition and precipitate radius, the number of growth layers is determined for each nucleus based on information from neighbouring cells. The thickness of the growth layer depends on the radius increment $\Delta r$ and the cell size. When the calculated layer thickness exceeds the cell dimension, neighbouring cells are incorporated into the precipitate and their states are updated. This stage corresponds to precipitate growth. The subsequent stage is precipitate coarsening, which involves the dissolution of smaller precipitates with radii below the critical radius and the growth of larger precipitates. The magnitude of the radius increment is calculated; negative values lead to a reduction in the number of precipitate layers, which may result in dissolution, whereas positive values correspond to precipitate growth. The transition rules applied in the CA model are based on the physical mechanisms of nucleation, growth and coarsening described by the kinetic model.

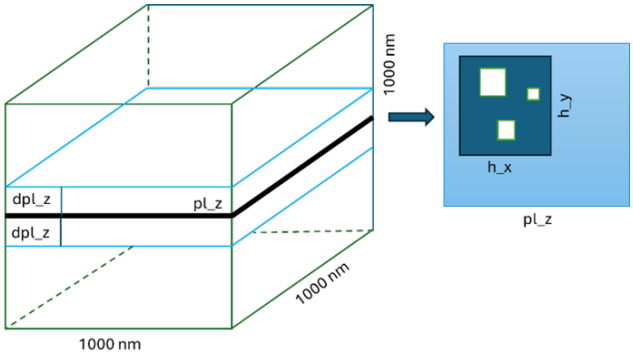



Fig. 2. Graphical presentation of the method of obtaining a image of carbonitride precipitate distributions

Fig. 2 presents a graphical illustration of the method used for simulating two-dimensional representations of carbonitride precipitate distributions. A cubic representative volume element with an edge length of *1000 nm* and a volume of $1\mu m^3$ ($1000^3\ nm^3$) is considered. The volume represents a selected region of the matrix containing precipitates. The variable $pl_z$ defines the position of the cross-sectional plane along the height of the computational domain. The half-thickness of the layer in which precipitates intersecting the observation plane are considered is defined by the variable $d_{pl_z}(pl_z \pm d_{pl_z})$. A fragment of the cross-sectional plane to be analysed is selected by specifying its dimensions $h_x$ and $h_y$, and the cellular automaton is defined within this area. The simulated precipitates located within the analysed region are subsequently visualized as a two-dimensional precipitate distribution.

The simulation of precipitate distributions using the cellular automata method is based on the random generation of precipitate nuclei and their spatial coordinates. The growth and coarsening processes are described using transition rules governing the evolution of the cellular automaton. The square appearance of precipitate cross-sections results from the discretization of the computational domain into square cells and from the adopted Moore neighbourhood, in which cells located along the edges and at the corners of a given cell are considered neighbours. Changes in the automaton state are stored in appropriate arrays. In the three-dimensional computational domain, precipitates are represented by sets of cubic cells. The generation of a two-dimensional precipitate distribution image involves determining the intersection between precipitates and the selected cross-sectional plane $pl_z$. If a precipitate intersects the observation plane, its cross-section is projected onto the resulting image. Due to the discretization adopted in the cellular automata model, the obtained precipitate cross-sections have a square shape, with dimensions determined by the current precipitate size and the cellular automaton parameters.

# 4. Experimental verification

Experimental studies were conducted on two types of heat-treatable steels containing V as a microalloying element and differing in nitrogen content: carbon–manganese (C–Mn) and carbon–chromium (C–Cr) steels [11, 21]. Both steels also contained small amounts of Ti and Nb. For simulations performed using the complex computational system, input data required for the calculations were obtained from the literature [13–23]. The chemical compositions of the investigated steels are presented in Table 1 (wt.%).

Table 1.
Chemical composition of steels, % mass

| steel | C | N | Nb | Ti | V | Mn | Si | Cr | Al |
|---|---|---|---|---|---|---|---|---|---|
| C-Cr | 0.41 | 0.0047 | 0.004 | 0.016 | 0.075 | 0.94 | 0.27 | 1.98 | 0.02 |
| C-Mn | 0.42 | 0.0046 | 0.02 | 0.011 | 0.26 | 1.47 | 0.33 | 0 | 0.011 |
| C-Mn | 0.44 | 0.0112 | 0.02 | 0.012 | 0.15 | 1.57 | 0.37 | 0 | 0.01 |

Samples 20×20×10mm were prepared and subjected to heat treatment. In the first stage, the samples were annealed in an electric tube furnace under a protective argon atmosphere at 1200°C for 1h to dissolve the carbonitride precipitates present in the steel. In the second stage, the furnace was allowed to cool naturally to 820°C for the C–Cr steel and 850°C for the C–Mn steels. The samples were then held isothermally for 20h, followed by water quenching.

A detailed microstructural analysis of the samples and carbonitride precipitates was performed using transmission electron microscopy (TEM). Thin foils and double-sided extraction replicas were prepared and examined using a JEOL JEM-200CX transmission electron microscope. Observations were carried out at magnifications ranging from 10.000-59.000x.

Fig. 3 shows microstructure images with revealed grain boundaries of former austenite in C-Cr steel, austenitized for 1 hour at temperatures 850, 1000, 1200°C and Fig. 4 for C-Mn and C-Mn(1) steels, austenitized for 1/2 hour at 1200°C and cooled freely in the furnace to 850°C and holding for 20 hours next with subsequent cooling in water.

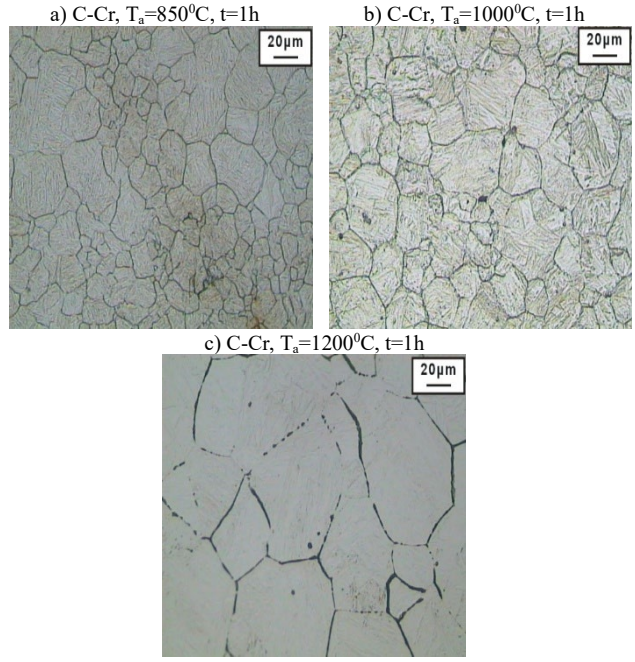



Fig. 3. Revealed grain boundaries of C-Cr steel for austenitizing temperatures of 850, 1000 and 1200°C for 1 hour

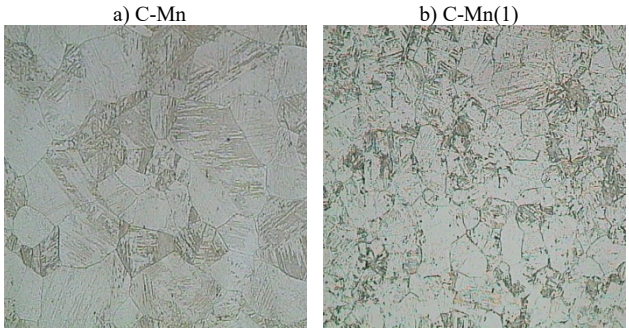



Fig. 4. Images of microstructures with revealed grain boundaries of C-Mn and C-Mn(1) steels

Fig. 3-4 present the experimentally observed prior austenite grain structures of the investigated steels after different heat-treatment conditions. These micrographs are included solely to characterize the experimental materials used for validation of the developed computational system and to illustrate the influence of heat treatment on the prior austenite grain structure. They are not intended to represent the results of the Cellular Automata (CA) model or to predict the final mechanical properties of the investigated steels. The CA simulation results, describing the spatial distribution of carbonitride precipitates within a representative austenite grain, are presented separately in Fig. 6–8. The principal objective of the present study is the validation of the precipitation model through comparison between experimentally observed and simulated precipitate distributions and their stereological parameters.

Between 6 and 20 TEM micrographs of precipitates were acquired for each steel, containing between 200 and 1000 precipitates in total. The micrographs exhibited significant contrast variations, which complicated the quantitative analysis of precipitate characteristics. Therefore, the original experimental images were re-analysed using newly developed image-processing and computational procedures, allowing a more accurate determination of the stereological parameters required for validation of the developed computational system. The quantitative analysis of carbonitride precipitates was performed using SigmaScan PRO 4.01, an original image-processing program developed by the authors, together with publicly available software, including MS Excel and GIMP. Images of thin foils and extraction replicas were additionally digitised to improve the quality and accuracy of the image analysis.

Fig. 5 compares the average precipitate radius obtained using three different approaches: the experimental data reported in [11, 21], manual image analysis using SigmaScan PRO, and simulations performed with the developed computational system. Its purpose is to validate the precipitation kinetics module of the developed computational system rather than to evaluate the final mechanical properties of the investigated steels. Fig. 6–8 present the precipitate distributions generated by the Cellular Automata (CA) module of the developed computational system together with the corresponding TEM micrographs and their processed versions used for quantitative analysis. Since carbonitride precipitates are only a few to several tens of nanometres in size, the CA simulations were performed for a single representative austenite grain. This approach enables direct comparison between the simulated precipitate distributions and the experimentally observed precipitates while focusing on the local precipitation process within an individual grain. Fig. 9 presents the empirical distributions of Feret diameters, whereas Fig. 10-11 show selected electron diffraction patterns together with their interpretation, confirming the crystallographic identification of the carbonitride precipitates.

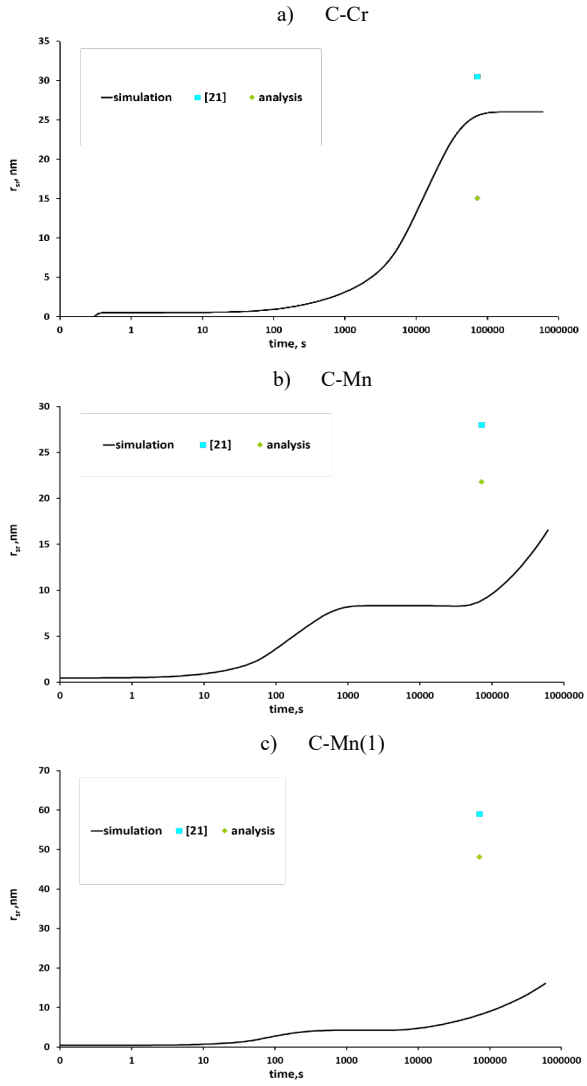



Fig. 5. Comparison of experimentally measured and simulated average carbonitride precipitate radius

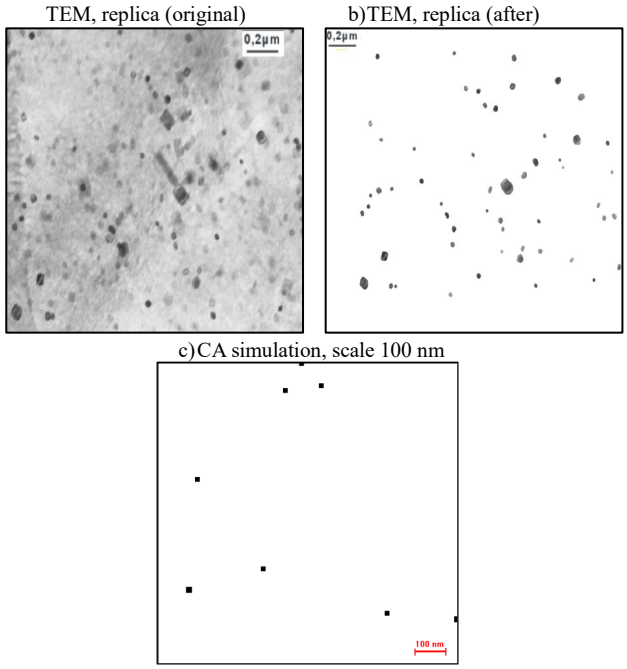



Fig. 6. Microstructure of C-Cr steel, after heat treatment (1200°C/1h/820°C/20h/$H_2O$)

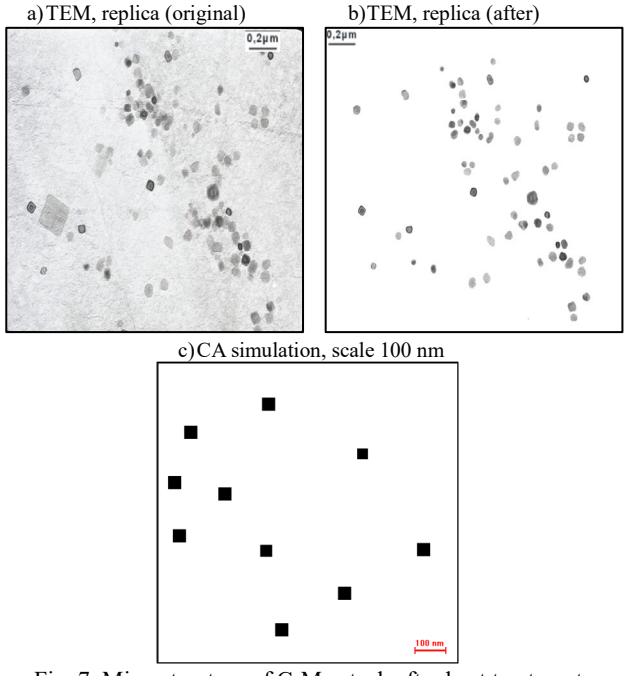



Fig. 7. Microstructure of C-Mn steel, after heat treatment (1200°C/1h/850°C/20h/$H_2O$)

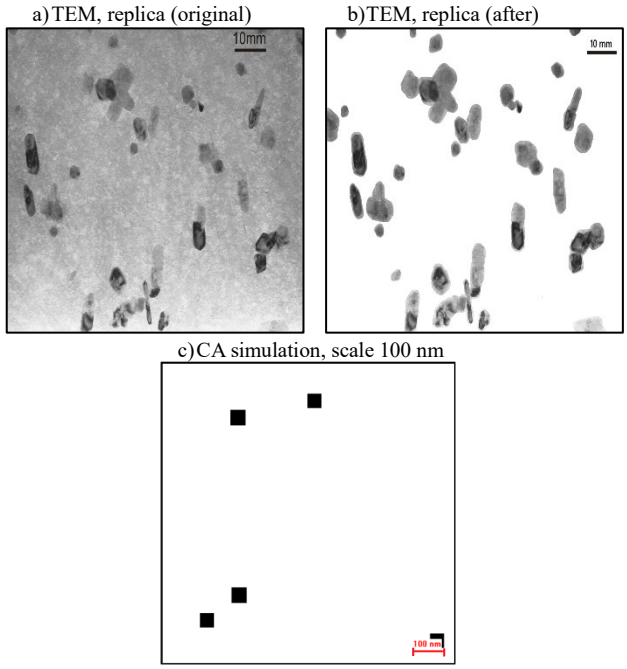
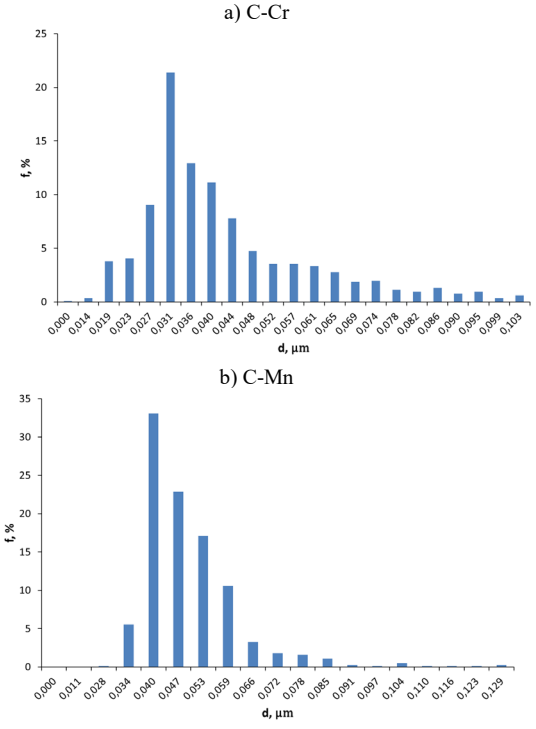



Fig. 8. Microstructure of C-Mn(1) steel, after heat treatment (1200°C/1h/850°C/20h/$H_2O$)



c) C-Mn(1)

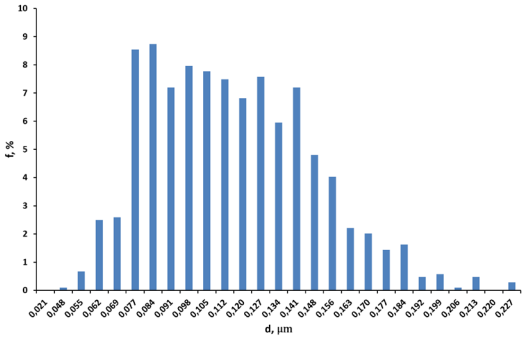
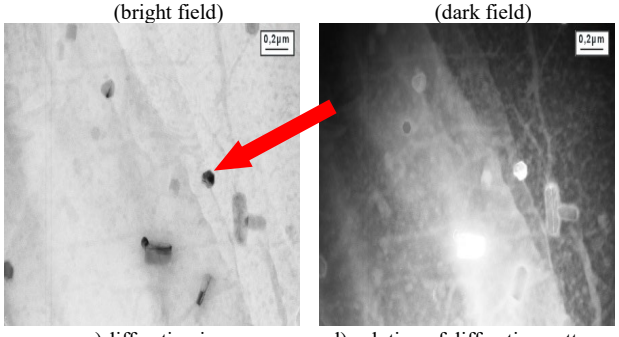


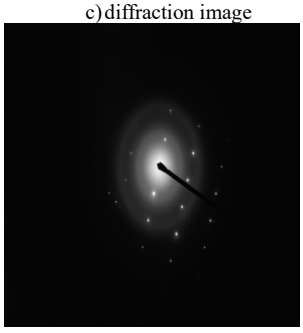

Fig. 9. Graphical presentation of Feret's diameter distributions of steels

a) microstructure (bright field)

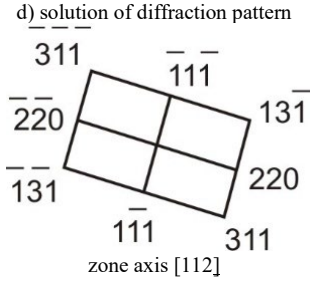
b) microstructure (dark field)




c) diffraction image



d) solution of diffraction pattern

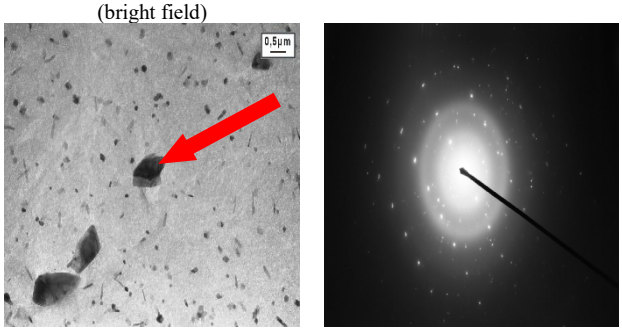



zone axis [112]

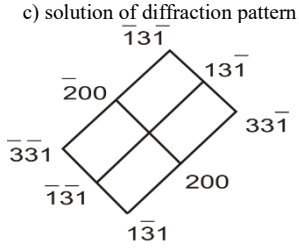
Fig. 10. Result of microscope analysis for C-Cr

a) microstructure (bright field)

b) diffraction image




c) solution of diffraction pattern




zone axis [013]

Fig. 11. Result of microscope analysis for C-Mn(1)

# 5. Results discussion

To explain the differences observed in the average precipitate radius, it is necessary to consider the heat-treatment procedure applied during sample preparation. The samples were heated in a tube furnace under a protective Ar atmosphere to an austenitizing temperature of $T_p = 1200\,℃$ and subsequently cooled in the furnace to $T_w = 850\,℃$ (C–Mn steels) or $820\,℃$ (C–Cr steel). Ideally, the samples should have been cooled rapidly from the austenitizing temperature to the isothermal holding temperature in order to suppress precipitation during cooling. However, this was not possible due to technical limitations of the experimental procedure. Consequently, carbonitride precipitation occurred during slow furnace cooling from $T_p = 1200\,℃$ to the holding temperature, resulting in a higher number of precipitates observed experimentally than those predicted by the developed computational model.

Carbonitride precipitates containing Ti, Nb and V, together with aluminium nitride precipitates, play an important role in the strengthening mechanisms of microalloyed steels. Due to their wide range of dissolution temperatures, these precipitates influence the microstructure through:

a. restricting austenite grain growth by pinning grain boundaries at elevated temperatures,
b. modifying recrystallization kinetics and phase transformation behaviour through the interaction of solute atoms and precipitates,
c. providing precipitation strengthening by forming fine carbonitride particles during cooling or isothermal holding.

Solute elements dissolved in austenite retard phase transformations and consequently increase the hardenability of steel. Accurate knowledge of the chemical composition of austenite together with the volume fraction, size and distribution of

undissolved precipitates is essential for describing precipitation behaviour and its influence on the evolving microstructure. These quantities may subsequently be used as input data for more comprehensive models predicting the mechanical properties of microalloyed steels.

Fig. 3–4 present the experimentally observed prior austenite grain structures of the investigated C–Cr, C–Mn and C–Mn(1) steels after the applied heat-treatment conditions. These micrographs are included solely to characterize the experimental materials used for validation of the developed computational system and to illustrate the effect of heat treatment on the prior austenite grain structure. They are not intended to validate the Cellular Automata (CA) model or to predict the final mechanical properties of the investigated steels. In the present study, the prior austenite grain structure is presented only as supplementary experimental information describing the investigated materials. The principal objective of the validation is the comparison between experimentally observed and simulated carbonitride precipitate distributions and their stereological parameters.

Fig. 5 compares the average carbonitride precipitate radius obtained using three different approaches: the experimental measurements reported in [21], the present image analysis, and simulations performed using the developed computational system. The purpose of this comparison is to validate the precipitation kinetics module by assessing its ability to reproduce the experimentally observed average precipitate size. In all analysed steels, the average precipitate radius reported in [21] is the highest. The present image analysis yields slightly lower values, which are generally in better agreement with the simulation results. Only for the C–Cr steel is the average precipitate radius obtained from the present image analysis lower than that predicted by the computational model.

Fig. 6–8 compare the precipitate distributions generated by the Cellular Automata module with the corresponding TEM observations. The agreement between the simulated and experimental precipitate distributions confirms that the proposed computational approach reproduces the main characteristics of the precipitation process. The remaining differences are mainly associated with precipitation occurring during slow furnace cooling prior to isothermal holding, which is not included in the present computational model.

The Feret diameter distributions (Fig. 9) are asymmetric and unimodal, with the modal values shifted towards smaller particle sizes. An increase in nitrogen content results in a reduction of the average precipitate radius, which is consistent with both the experimental observations and the simulation results.

Fig. 10-11 present representative electron diffraction patterns together with their interpretation, confirming the crystallographic identification of the carbonitride precipitates observed in the investigated steels.

# 6. Conclusions

The verification of the developed computational system against the experimental data presented in this work demonstrates that the Cellular Automata (CA) module, coupled with the thermodynamic and kinetic models, is capable of reproducing the spatial distribution and stereological characteristics of carbonitride precipitates with satisfactory accuracy. The adopted physicochemical parameters provide simulation results that are in good agreement with the experimental observations.

The developed computational system enables the simulation of carbonitride precipitation and the generation of two-dimensional images of precipitate distributions, which can be directly compared with transmission electron microscopy (TEM) observations. Relatively few studies have reported numerical simulation of precipitate distributions in microalloyed steels; therefore, further experimental investigations are required to provide additional high-quality data for comprehensive validation of the proposed approach.

Carbonitride precipitates play a dual role in microalloyed steels by restricting austenite grain growth at elevated temperatures and contributing to precipitation strengthening after phase transformation. Their stereological characteristics, particularly the precipitate size distribution and volume fraction, are important descriptors of the precipitation process and may be determined using the developed computational system.

The developed computational system provides quantitative information on carbonitride precipitation behaviour and precipitate stereological parameters based on the chemical composition of steel and heat-treatment conditions. These results may be used as input data for more comprehensive models describing the evolution of the final microstructure and predicting mechanical properties. The prediction of mechanical properties itself is beyond the scope of the present work and requires additional information concerning the matrix microstructure and other strengthening mechanisms.

Further development of the computational system should include:

a) extension of the model to steels containing multiple microalloying additions,
b) validation using a broader experimental database covering a wider range of chemical compositions and processing conditions,
c) coupling of the precipitation model with microstructure evolution and mechanical property prediction models.

# Acknowledgements

The work was realized as a part of fundamental research financed by the Ministry of Science and Higher Education, grant no. 16.16.110.663.

# References

[1] Goldschmidt, H.J. (1967). *Interstitial Alloys*. London: Butterworths.
[2] Adrian, H. (1992). Thermodynamic model for precipitation of carbonitrides in high strength low alloyed steels up to three microalloying elements with or without additions of aluminum. *Materials Science and Technology*. 8, 406-420. https://doi.org/10.1179/mst.1992.8.5.40.
[3] Liu, W. & Jonas, J.J. (1989). Calculation of the Ti(CyN1-y) - Ti4C2S2 - MnS austenite equilibrium in Ti-bearing steels. *Metallurgical Transactions A*. 20A, 1361-74. https://doi.org/10.1007/BF02665494.

[4] Roberts, W., Sandberg, A. (1980). *The composition of V(C, N) as precipitated in HSLA steels microalloyed with vanadium,* Report no. IM-1489, Swedish Institute for Metals Research.
[5] Speer, J.G., Michael, J.R. & Hansen, S.S. (1987). Carbonitride precipitation in niobium/vanadium microalloyed steels. *Metallurgical Transactions A*. 18A, 211-222. https://doi.org/10.1007/BF02825702.
[6] Adrian, H., Augustyn-Pieniążek, J., Marynowski, P. & Matusiewicz, P. (2014). The kinetic model of the carbonitrides precipitation process in microalloyed steels. *Hutnik-Wiadomości Hutnicze*. 81(4), 208-214. (in Polish).
[7] Marynowski, P., Adrian, H. & Głowacki, M. (2019). Modeling of the kinetics of carbonitride precipitation process in high-strength low-alloy steels using cellular automata method. *Journal of Materials Engineering and Performance*. 28(7), 4018-4025. https://doi.org/10.1007/s11665-019-04170-4.
[8] Wagner, R., Kampmann, R. (1991). *Material science and technology: a comprehensive treatment*. Jon Wille & Sons Inc.
[9] Marynowski, P. & Hojny M. (2026). The influence of the thermodynamic equilibrium model of the Fe-M-C-N system on the results of calculations of carbonitride precipitation kinetics. *Archives of Foundry Engineering.* 26(2), 191-198. https://doi.org/10.24425/afe.2026.158006 .
[10] Adrian, H. (2011). *Numerical modelling of heat treatment processes.* Kraków: Wydawnictwa AGH. (in Polish).
[11] Marynowski, P. (2021). *Modelling of the kinetics of carbonitride precipitation process in high-strength low-alloy steels using cellular automata method.* Doctoral dissertation. AGH Kraków. (in Polish).
[12] Marynowski, P., Hojny, M. & Dębiński, T. (2023). The effect of microalloying (Nb, V) and interstitial (C, N) elements on mechanical properties of microalloyed steels. *Archives of Foundry Engineering.* 23(4), 127-136. DOI: 10.24425/afe.2023.146687.
[13] Robson J.D. (2004). Modelling the overlap of nucleation, growth and coarsening during precipitation*. Acta Materialia*. 52, 4669-4676. DOI: 10.1016/j.actamat.2004.06.024.
[14] Hillert M., Staffansson L.I., (1970). The regular solution model for stoichiometric phases and ionic melts. *Acta Chemica Scandinavica.* 24, 3618-3626.
[15] Maugis, P., Goune, P., Barges, D., Dougnac, D., Ravaine, M., Lamberigts, T., Siwecki, T. & Bi, Y. (2003). A model for niobium carbonitride precipitation in ferrite. *Materials Science Forum*. 426-432, 1313-1318.
[16] Haynes WM (Eds.). (2017). *CRC Handbook of Chemistry and Physics 97th Edition.* Boca Raton USA.
[17] Goldschmidt, H.J. (1967). *Interstitial Alloys*. Butterworth.
[18] Maugis, P. & Goune, M. (2005). Kinetics of vanadium carbonitride precipitation in steel: A computer model*. Acta Materialia*. 53, 3359-3367. DOI: 10.1016/j.actamat.2005.03.036.
[19] Perez, M. (2008). Gibbs-Thomson effects in phase transformations. *Scripta Materialia.* 52, 2119-2131.
[20] Bołd, T., Kuziak, B., Tokarz, A. & Yi-Wen, Ch. (1993). Low-alloy steels containing titanium, vanadium and nitrogen for sections and forgings*. Hutnik–Wiadomości Hutnicze.* 4, 114-129. (in Polish).
[21] Głowacz, E. (2013). *A kinetic model for the precipitation of nitrides in microalloyed steels with varying nitrogen content*. Doctoral dissertation. AGH Kraków. (in Polish).
[22] Marynowski, P., Adrian, H. & Głowacki, M. (2018). Cellular Automata model of carbonitrides precipitation process in steels*. Computer Methods in Materials Science.* 18(4), 120-128. ISSN (1641-8581).
[23] Marynowski, P., Adrian, H. & Głowacki, M. (2013). Cellular automata model of precipitation in microalloyed niobium steels*. Computer Methods in Materials Science*. 13(4), 452-459.